Spatial patterns in phytoplankton community composition and their relationship to carbon export on the northwest Weddell Sea continental shelf

Meredith G. Meyer[1], Robert J. W. Brewin[2], Xuerong Sun[2], Clara Manno[3], Florence Atherden[3], Sasha J. Kramer[4], Giorgio Dall'Olmo[5], and Karen J. Heywood[1]

[1]Centre for Ocean and Atmospheric Sciences, School of Environmental Sciences, University of East Anglia, Norwich, UK
[2] Centre for Geography and Environmental Science, Department of Earth and Environmental Sciences, University of Exeter, Penryn, UK
[3]British Antarctic Survey, Cambridge, UK
[4] Department of Earth & Environment, Boston University, Boston, MA, USA
[5]Istituto Nazionale di Oceanografia e di Geofisica Sperimentale, Trieste, Italy

Correspondence to: Meredith G. Meyer (m.meyer@uea.ac.uk)

Abstract. Typically, diatoms, haptophytes, and cryptophytes dominate phytoplankton biomass and abundance in the Southern Ocean, determining bloom dynamics and carbon transfer and responding to physical factors such as sea ice concentration and mixing. However, phytoplankton community composition remains understudied in many regions of the Southern Ocean. Here, we present pigment-based phytoplankton community-composition data from a summer cruise to the northwest Weddell Sea continental shelf. Our pigment and diagnostic pigment analysis results show a predominance of fucoxanthin and 19'-hexanolyoxyfucoxanthin, i.e., diatoms and haptophytes, throughout various oceanic regimes and water column depths, consistent with community compositions from similar cold continental shelf regions. These are some of the only pigment-based community composition data from this key region for deep-water formation and carbon transport. Taken together, the relative biomass of the three dominant phytoplankton groups (39.7% diatoms, 30.2% haptophytes, and 14.9% cryptophytes) explain the majority (R^2 = 0.37 – 0.82) of carbon export to 150 m. While additional measurements are needed to verify these relationships, these findings highlight the need to consider frequently overlooked phytoplankton types, alongside diatoms, in Southern Ocean models of carbon export due to the key, but differing, roles these groups play in production-export dynamics.

1 Introduction

Phytoplankton community composition is a key driver in nutrient cycling, primary production, and carbon export across the ocean (Henson et al., 2021; Kramer et al., 2025). There is currently increased attention on the role of phytoplankton taxonomy in ocean processes with recent studies showing that climate change has already begun to shift phytoplankton abundance (Hong et al., 2025) and taxonomic patterns worldwide (Anderson et al., 2021; Cael et al., 2021; Xi et al., 2025). This trend is expected to continue with a restructuring of phytoplankton taxa in coming decades (Henson et al., 2021). In the

Deleted: influence on

Deleted:

Deleted: To our knowledge,

Deleted: t

Deleted: .

Deleted: T

Deleted: 1

Southern Ocean, some of these transitions appear to be linked to physical drivers, such as sea-ice concentration (Hayward et al., 2025), but evaluating the impacts of these shifts in ocean biogeochemistry and ecosystem functioning is complicated by regional differences and substantial interannual variability (Deppler and Davidson, 2017), making the need for regional measurements critical.

Despite its importance, phytoplankton community composition remains an understudied oceanographic indicator that is difficult to measure on large scales. The increase in hyperspectral capabilities on satellites (Gorman et al., 2019) and remotely-operated instruments (Suomalainen et al., 2021) has been instrumental in increasing the amount of phytoplankton community composition data collection to a level previously not possible (Dierssen et al., 2021; Kramer et al., 2022; Cetinić et al., 2024; IOCCG, 2026). The launch of the NASA Plankton, Aerosol, Cloud, ocean Ecosystem (PACE) satellite was the biggest step forward to date toward achieving global, hyperspectral ocean colour data (Gorman et al., 2019). However, retrieving phytoplankton taxonomy from satellites relies on constructing relationships between remote sensing reflectance (R_{rs}) and phytoplankton community composition that must be validated by in-situ measurements (Sathyendranath et al., 2014). Currently, high performance liquid chromatography (HPLC) remains the standard by which phytoplankton pigments are measured and these R_{rs}-based models are validated, but the human sampling effort, cost, and analytical precision required for HPLC analysis limit the number of datasets that exist, particularly in remote regions such as the Southern Ocean.

Hayward et al. (2025) compiled HPLC datasets from the Southern Ocean (n = 14,824 samples), but their comprehensive dataset contains no HPLC samples from the Weddell Sea continental shelf. The phytoplankton community composition data that are available on high-latitude Antarctic continental shelves are highly biased towards the Western Antarctic Peninsula where repeat monitoring programs (Smith et al., 1995; Venables et al., 2023) enable data collection. Phytoplankton community composition sampling in the ice-heavy Weddell Sea is sparse, with most of our knowledge coming from several independent cruise programs occurring broadly in the Weddell Sea sector of the Southern Ocean, over varying months and years (Kang and Fryxell, 1993; Schloss and Estrada, 1994; Wright et al., 2009; Xi et al., 2020; Flynn et al., 2023). Here, we present results from 50 HPLC samples collected throughout the water column, and a few collected from melted sea ice, to investigate the spatial patterns of dominant phytoplankton groups and how these patterns compare with physical parameters and to POC flux across previously unsampled regions of the Weddell Sea continental shelf and slope region as part of the Processes Influencing Carbon Cycling: Observations of the Lower limb of the Antarctic Overturning (PICCOLO) project (Heywood and Bell, 2024). The patterns and relationships presented here provide novel understanding of phytoplankton community composition as it relates to carbon cycling within and out of the surface ocean in this important region for Southern Ocean deep-water formation.

Deleted: , Bracher et al., 2017; Chase et al., 2017, Lange et al., 2020, Kramer et al., 2022

Deleted:

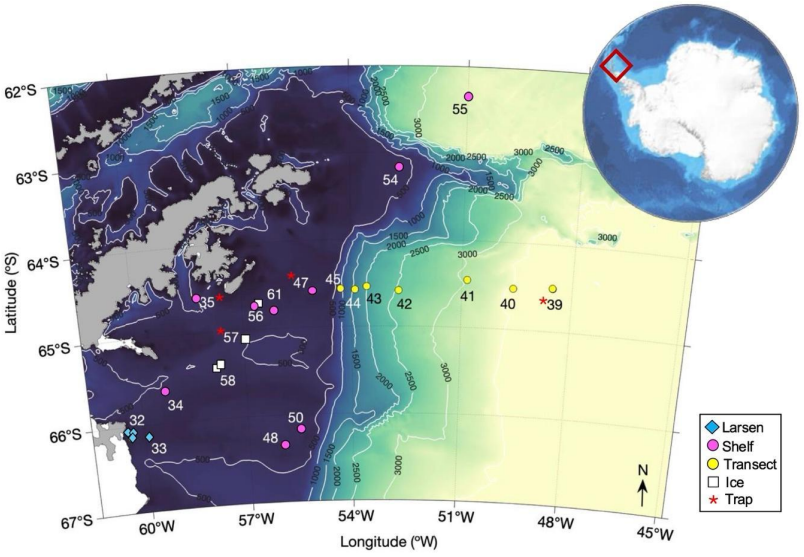
Deleted: gram

2 Methods

2.1 Cruise overview

The PICCOLO cruise (SD035) occurred from 17 January (yearday (YD) 17) to 9 March (YD 69) 2024 aboard the *Royal Research Ship (RRS) Sir David Attenborough* in the northwest Weddell Sea region of the Southern Ocean (Heywood

and Bell, 2024). The ship sampled across multiple, different oceanic regimes (Figure 1) which can be classified as on the continental shelf and close to the Larsen-C Ice Shelf ("Larsen"; YD 32-33, blue diamonds), on the continental shelf elsewhere ("shelf"; YD 47, 49, 55, 61, 129-134, pink circles), from a zonal transect sampling crossing the continental slope ("transect"; YD 40-45, yellow circles), and on the continental shelf and near (approximately 0-200 m) to sea ice ("ice"; YD 48-50, 56-58; white squares. Sometimes multiple CTD casts occurred on the same YD. These CTD casts are presented individually to show the greatest amount of geographic variability. The Larsen samples were collected from a polynya that opened shortly before collection and proceeded to close shortly after collection. Water column samples were predominantly collected via a CTD rosette equipped with a Sea-Bird SBE 911+ CTD profiler, but some samples were collected from the underway system, which has a seawater intake at approximately 7 m depth. Sea ice samples were collected from either melted sea ice cores, in one case a particularly biomass-rich chunk of sampled ice, termed "brown ice", or water pumped from the sea ice-ocean interface. HPLC pigment samples were collected from all regimes with water column depths ranging 3 – 100 m. All HPLC samples were collected within the euphotic zone (measured as 1% of surface irradiance from the CTD-mounted PAR sensor) which ranged from 23 – 100 m with an average of 55 ± 21 m. A drifting sediment trap was deployed for 11-22 hours at 4 locations spanning the continental shelf and open ocean environments (YDs 35, 39, 47, 57; red stars in Figure 1). For full details on collection dates and locations, see Table S1.



Deleted: -derived water

Deleted:

Deleted:

Deleted: The

Deleted:

Deleted: The euphotic zone (measured as 1% of surface irradiance) ranged from 23 – 100 m with an average of 55 ± 21 m.

Figure 1. Map of HPLC sample locations by yearday (YD) of sampling. Global inset shows the location of sampling within the Southern Ocean generally. Isobaths are shown in white. During trap deployments, POC samples were taken at 50, 100, and 150 m depth.

2.2 High Performance Liquid Chromatography Pigment Concentrations

For the underway sampling, in addition to bulk water samples, size-fractionated HPLC pigment samples were collected by passing seawater through cartridge filters that isolate distinct size classes (here, <25 µm and <3 µm; Polygard CR cartridge filters). For all samples, 360–2000 mL of seawater was filtered through Whatman GF/F glass microfiber filters (0.7 µm nominal pore size, 25 mm diameter) under low vacuum pressure. Filters were placed in cryovials, flash-frozen in liquid nitrogen, and stored at −80 °C until onshore transport and subsequent analysis.

Filters were shipped to DHI Analytics where they were analysed according to the method of Van Heukelem and Thomas (2001). HPLC results were analysed for key accessory pigments including: alpha-beta-carotene (a-b caro), total chlorophyll b, zeaxanthin, diatoxanthin, alloxanthin, diadinoxanthin, 19'-hexanoyloxyfucoxanthin (hex-fuco), fucoxanthin, 19'-butanoyloxyfucoxanthin (but-fuco), peridinin, total chlorophyll c, and total chlorophyll a. The analytical limit of detection for this analysis ranged between 0.0003 – 0.0006 µg L^{-1} with a coefficient of variation of 0.22% for this dataset. Pigments concentrations below the detection limit were set to zero. Proportional contributions of each key accessory pigment were calculated as shown in the following equation (1):

$$Proportional\ contribution\ (\%) = \frac{accessory\ pigment\ concentration}{\sum all\ accessory\ pigment\ concentrations} \quad (1)$$

Where the concentration of each key pigment is divided by the sum of the total concentration of all accessory pigments. A table of accessory pigment distribution relative to dominant phytoplankton functional types are included in the Supplemental Material.

2.3 *Phytoclass* Analysis

To estimate phytoplankton community composition, HPLC data were analysed via the R program *phytoclass* (phytoclass.github.io/phytoclass/; Hayward et al., 2023). This model is specific to the Southern Ocean and assesses the distribution of diatoms, dinoflagellates, haptophytes, cryptophytes, and *Synechococcus* from simulated annealing of accessory pigment concentrations (Hayward et al., 2023). *phytoclass* uses the same basis and statistical assumptions as the CHEMTAX method (Mackey et al., 1996) but is tuned for the Southern Ocean. While both of these methods make assumptions about the relationships between and among phytoplankton pigments that are not upheld in statistical analyses of pigment-based datasets (Kramer and Siegel, 2019), CHEMTAX has historically shown good agreement with microscopy and 18S rRNA gene sequencing data from the Western Antarctic Peninsula (e.g., Lin et al., 2019; Brown et al., 2019; Lin et al., 2021). Emerging studies have also shown general agreement between *phytoclass* outputs with microscopy and Flowcam data in open-ocean

Deleted: **Figure 1.** Map of HPLC sample locations by yearday of sampling. Global inset shows the location of sampling within the Southern Ocean generally. Isobaths are shown in white.

Deleted: HPLC pigment samples were collected from both discrete water column depths (ranging 3 – 120 m) and the ship's underway system, which has a seawater intake at approximately 7 m depth.

Formatted: Font: (Default) +Body (Times New Roman)

Formatted: Font: (Default) +Body (Times New Roman)

Deleted: by dividing

Deleted: A

Deleted: , and analysis specific information

Deleted: Southern Ocean-trained

Deleted: is based on a similar approach to the

regions of the Southern Ocean, providing enhanced confidence in applying the method in this ecosystem (T. Ryan-Keogh, personal communication). *phytoclass* and HPLC results are divided into surface (<20 m), mid-water (20 – 49 m), and deep samples (50 – 100 m).

2.4 Particulate Organic Carbon Flux

Particulate organic carbon (POC) was collected from a drifting sediment trap with three collection carousels at 50, 100, and 150 m. This design enables one trap containing three separate carousels with collection canisters (for seawater) at each depth. Upon drifting sediment trap recovery, a messenger was released, triggering a custom closing mechanism and preventing contamination and potential overestimation of the flux as the trap was hauled onboard. Once onboard, the trap material was processed immediately.

For processing, the collection canisters were descended into carboys, thoroughly mixed, and 600 ml of collected water was filtered onto pre-combusted (450°C, 16 hrs), pre-weighed 25 mm Whatman glass fibre filters (0.45 µm pore size, air dried for 24 hours) and frozen at -20ºC until onshore analysis at the British Antarctic Survey. POC samples were fumed for 24 hours with 37% HCl in a desiccator and placed in sterile nickel capsules. POC samples were then analysed and blank corrected using a CE Instruments NA2500 elemental analyser which was calibrated using an acetanilide calibration standard with a known % C and % N (71.09 % and 10.36 % respectively). Rates of POC flux were calculated according to the following equation (2):

$$Flux = \frac{POC}{A * d}$$

Where POC is the concentration of particulate organic carbon, A is the area of the cannister opening, and d is trap duration (days). For full details, see Atherden et al. (2026).

2.5 Phytoplankton Community Composition vs. POC Flux Analysis

HPLC results were compared with particulate organic carbon (POC) flux measured via sediment traps, following a similar analysis to that of Kramer et al. (2025). In their analysis, those authors compared POC flux with the summed relative sequence abundance of diatoms + photosynthetic hacrobia (haptophytes and cryptophytes) / all other phytoplankton groups (in that study, chlorophytes and dinoflagellates) using metabarcoding data (18S rRNA gene V4 region). Kramer et al. (2025) decided to separate diatoms and hacrobia from all other phytoplankton after testing the statistical power of six pigment-based eukaryotic phytoplankton groups to reconstruct POC flux. Here, we follow a similar approach, combining the diatom, haptophyte, and cryptophyte percent contribution relative to dinoflagellate and *Synechococcus* percent contributions from pigments in surface samples (≤10 m) using the *phytoclass* output according to the following equation (3):

$$PCC_{ratio} = (\text{Diatoms} + \text{Haptophytes} + \text{Cryptophytes}) / (\text{Dinoflagellates} + \textit{Synechococcus}) \quad (3)$$

Formatted: Font: Italic

Moved up [2]: The trap was deployed for 11-22 hours at 4 locations spanning the continental shelf and open ocean environments (red stars in Figure 1).

Formatted: Indent: First line: 0 cm

Deleted: rates of

Deleted: e

Deleted: e

Deleted: eq

Deleted: 1

Deleted: 1

where PCC_{ratio} stands for diagnostic phytoplankton community composition. For this analysis, dinoflagellates and *Synechococcus* represent the remaining phytoplankton groups based on the *phytoclass* designation. POC fluxes from four drifting sediment traps were compared with co-located HPLC samples from the YD 35 (shelf), YD 39 (transect), YD 47 (shelf), and YD 57 (ice) locations.

2.6 Method Uncertainties

Phytoplankton accessory pigment analysis has inherent uncertainty for interpreting taxonomy due to (1) the large fraction of accessory pigments shared between broad phytoplankton groups, (2) the relatively plastic nature of phytoplankton pigments in response to changes in nutrient and light regimes, and (3) the high degree of co-linearity between all phytoplankton pigments, which is a violated assumption of many popular pigment-based algorithms such as CHEMTAX and *phytoclass* (Kramer and Siegel, 2019). For example, for *Phaeocystis*, an important Southern Ocean taxon, shared pigments can confound the interpretation of assemblages which may be either *Phaeocystis* or dinoflagellates based on traditional CHEMTAX methods (Mendes et al., 2018). However, HPLC pigments remain the gold standard for developing and validating ocean colour algorithms, so examining relationships between POC flux and pigment-based phytoplankton groups enhances potential for improving remotely-sensed export models. Further, HPLC pigment-based phytoplankton groups broadly compare well with other metrics for determining phytoplankton community composition across numerous coastal and open ocean ecosystems (e.g., Garibotti et al., 2003; Lin et al., 2019; Kramer et al., 2024). Additionally, certain methodological caveats may be introduced by the differences in methods between this study and Kramer et al. (2025), namely the use of HPLC pigments instead of gene-based community composition, and the difference (~40-45 m) in depth and collection time (hours) between our surface seawater HPLC samples and our sediment trap POC flux samples. For the work by Kramer et al. (2025), the rRNA gene samples were collected directly from the sediment trap, which was deployed for an average of 2-4 days, alongside the POC flux samples. In this study, rates of POC flux were paired with HPLC samples that were co-located upon trap recovery. The sediment traps travelled varying distances (between 1 and 5 km; Figure S2) between deployment and recovery and thus include some spatial biases in flux. For two trap deployments, CTD casts occurred before and soon after deployment allowing for the assessment of absolute salinity, conservative temperature, and fluorescence which showed minimal change before and after deployment (Figure S3). Despite these broad differences, the methods used here still allow for the relative contribution of pigment-based PCC_{ratio} to be assessed as a potential indicator of POC flux (i.e., carbon export) magnitude across sampling depths.

3 Results and Discussion

3.1 Overarching Phytoplankton Community Distribution

Throughout the region, total chlorophyll *a* ranged from 0.06 – 3.4 μg L^{-1} for water column samples (Figure 2). There appears to be evidence of a subsurface chlorophyll maxima with the peak concentrations for total samples in the 20 – 49 m

Deleted: (2025)decided

Deleted: testing the statistical power of six pigment-based eukaryotic phytoplankton groups to reconstruct POC flux.

Deleted: export

Formatted: Font: Italic

Formatted: Font: Italic

Deleted: YD 47 (shelf),

Deleted: See supplemental material for a full discussion on the considerations and uncertainty associated with pigment-based community composition.

Formatted: Font: Italic

Formatted: Font: Italic

Deleted: ¶

range (3.4 µg L^{-1}) exceeding that of surface samples (1.9 µg L^{-1}; Figure 2). Across all samples, the proportionally dominant pigments were fucoxanthin, hex-fuco, and chlorophyll c with variable, but sometimes high, percent contributions of alloxanthin and chlorophyll b (Figure 3). Broadly, this finding is consistent with previous HPLC studies which found the community in the Weddell Sea open-ocean region to be dominated by diatoms (fucoxanthin and chlorophyll c), haptophytes (hex-fuco, but-fuco, fucoxanthin, and chlorophyll c), and cryptophytes (alloxanthin; Wright et al., 2010; Hayward et al., 2025). Accordingly, the *phytoclass* output found a predominance of diatoms (mean = 40 ± 26%) followed closely by haptophytes (30 ± 22%) and cryptophytes (15 ± 24%) across the dataset (Figure 3). *Synechococcus* made up a non-negligible fraction with a mean percent contribution of 13 ± 10%. However caution should be taken with this finding because, while *Synechococcus* can be found in the Southern Ocean, they are more commonly associated with lower latitudes and the results may be skewed due to the sharing of zeaxanthin between *Synechococcus* and haptophytes (Hayward et al., 2023; Hayward et al., 2024). The pigments exhibited strong spatial variability, with haptophytes dominating at the Larsen-C Ice Shelf locations while diatoms dominated in the ice core and interface samples and at most non-Larsen water column locations (Figure 3G-J). Cryptophytes exhibited temporal variability, increasing in contribution towards the end of the cruise on YD 58 and 61 (Figure 3).

Deleted: 2

Deleted: 2

Deleted: ,

Deleted: 2

Deleted: 2

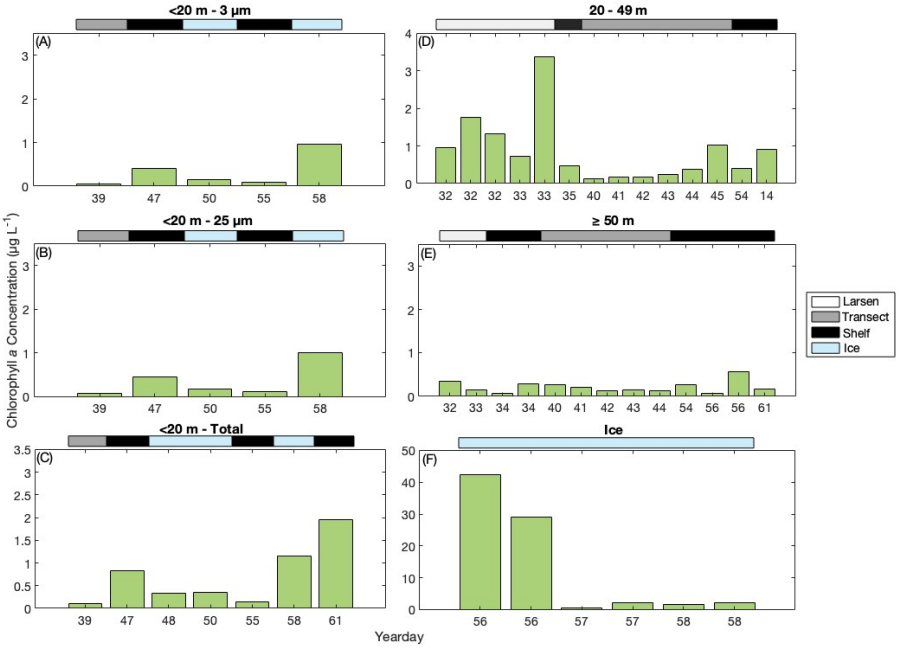


Figure 2. Total chlorophyll *a* concentrations from HPLC analysis (µg L^{-1}; C, D) for all samples by depth and yearday (YD). Most of the samples collected from <20 m were size fractionated, producing 3 (A), 25 (B), and total (C) concentrations. All other samples (D-F) were whole seawater (total) samples. Sea ice samples are shown separately to visualise higher concentrations. On some YDs, multiple samples were collected.

Deleted: 2

Formatted: Font: Italic

Formatted: Superscript

Deleted: Percent contribution (%) of HPLC-derived accessory pigments by depth of sampling and yearday. Samples collected from <20 m were size fractionated, producing 3 (A-B), 25 (C-D), and total (E-F) concentrations. All other samples (-) were whole seawater (total) samples. Accessory pigment abbreviations stand for alpha-beta-carotene (a-b caro), chlorophyll b (chl b), zeaxanthin (zeax), diatoxanthin (diatox), alloxanthin (allo), diadinoxanthin (diadino), 19'-hexanolyoxyfucoxanthin (hex-fuco), fucoxanthin (fuco), 19'-butanolyoxyfucoxanthin (but-fuco), peridinin (peridin), and chlorophyll c (chl c).

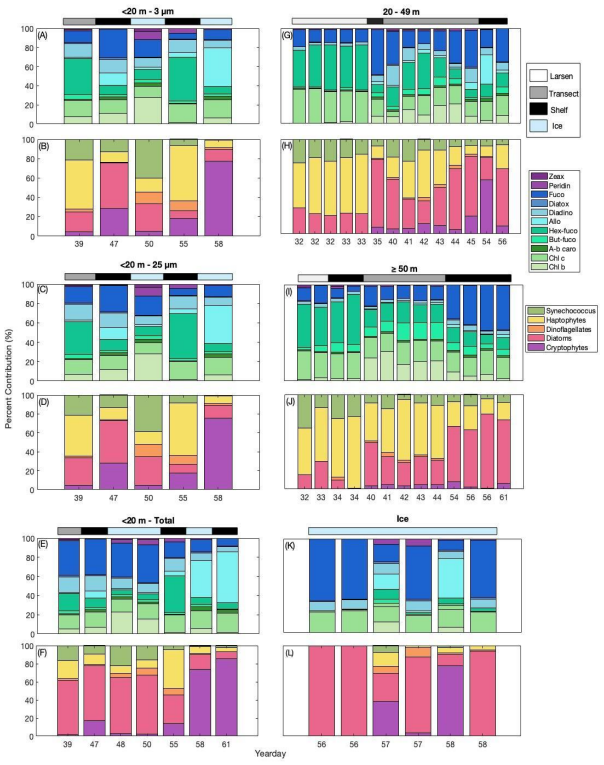


Figure 3. Percent contribution (%) of HPLC-derived accessory pigments to total accessory pigments by depth of sampling and yearday. Samples collected from <20 m were partially size fractionated, producing 3 (A-B), 25 (C-D), and total (E-F) concentrations. All other samples were whole seawater (total) samples. Accessory pigment abbreviations stand for alpha-beta-carotene (a-b caro), chlorophyll b (chl b), zeaxanthin (zeax), diatoxanthin (diatox), alloxanthin (allo), diadinoxanthin (diadino), 19'-hexanolyoxyfucoxanthin (hex-fuco), fucoxanthin (fuco), 19'-butanolyoxyfucoxanthin (but-fuco), peridinin (peridin), and chlorophyll c (chl c).

Deleted: (-)

These data (Figure 3) show multiple phytoplankton groups coexisting in a mixed assemblage with the absence of a substantive phytoplankton bloom during most of the expedition (Figure 2). Many studies have shown that climate change is already having noteworthy and nonuniform impacts with substantial taxonomic shifts on phytoplankton blooms across the Southern Ocean (Thomalla et al., 2023; Hayward et al., 2025). This would suggest our findings should be interpreted in light of this changing environment. They represent the bloom in 2024 and may differ from the average conditions decades ago. Studies from the marginal ice zone of the Weddell Sea suggest phytoplankton blooms peak prior to mid-January, but climate change induced declines in ice concentration has been shown to cause earlier bloom initiation and later termination for regions that previously experienced substantial ice cover (Thomalla et al., 2023). Thus, historical and recent studies supports the assumption that our February-March samples represent bloom decline conditions. The exceptions to this interpretation were the samples collected at the Larsen-C Ice Shelf, discussed below.

These pigment concentration patterns and *phytoclass* output (Figure 2; Figure 3) provide new insight on the region's ecosystem structure and biogeochemical processes as well as motivation for future investigations of the region using advanced technology, including hyperspectral satellites such as PACE. Our results provide quantifiable relationships between key phytoplankton groups and indicate co-location of diatoms, haptophytes, and cryptophytes in nearly all samples, throughout the upper 100 m (Figure 3). However, size fraction and depth patterns exist with haptophytes accounting for a larger proportion of pigments in the smaller size fractions and higher proportions of haptophytes and cryptophytes at the surface to mid-water column (Figure 3A-F; discussed further below). Additionally, the current impact of the PACE satellite is limited by validation data, namely HPLC samples, in remote regions, particularly at high latitudes (Cetinic et al., 2024). The pigment algorithms being implemented by NASA for PACE (Chase et al., 2017; Kramer et al., 2022) were trained and validated only with HPLC data collected between 60S - 60N. The new data presented here represent one of the only HPLC datasets and one of the only phytoplankton community composition datasets from the Weddell Sea continental shelf. Therefore, these data provide valuable information to improve current pigment algorithms, without which satellite retrievals in this region will continue to be misrepresented (Chen et al., 2021; Xi et al., 2025).

3.2 The Larsen-C Ice Shelf Bloom

The Larsen-C Ice Shelf samples (n = 7; YD 32 and 33) were notably different from the rest of the samples. Both mid-water (20 – 49 m) and deep (50 – 100 m) samples were dominated by hex-fuco, which comprised on average 44 ± 3% of total accessory pigments (Figure 3). Additionally, in this region, fucoxanthin displayed its lowest percent contribution (average = 15 ± 2%) to total accessory pigments of the entire dataset (Figure 3). The proportional increase of hex-fuco and decrease of fucoxanthin concentrations were both significant (P-value < 0.05) and corresponded to a substantial increase in hex-fuco with average Larsen-C concentrations of 0.64 ± 0.64 µg L^{-1} (relative to the total sample average of 0.13 ± 0.31 µg L^{-1}) as well as a substantial decrease in fucoxanthin with average Larsen-C concentrations of 0.19 ± 0.17 µg L^{-1} (relative to the total sample average of 1.1 ± 4.6 µg L^{-1}). These changes in pigment concentration and fucoxanthin and hex-fuco pigment proportions,

Deleted: HPLC chlorophyll *a* concentrations, without Larsen-C samples, ranged from 0.06 - 2.0 µg L^{-1}

Deleted:

Deleted: While the phytoplankton bloom succession in this region is poorly documented,

Deleted: s

Deleted: s

Deleted: suggesting

Deleted: ?

Deleted: (von Berg et al., 2020)

Deleted: s

Deleted: ?

Deleted: important advances for both our

Deleted: understanding

Deleted: of

Deleted: ??

Deleted: at all depths

Deleted: ?

Deleted: 2

Deleted: These

Deleted: , if not the only,

Deleted: , generally,

Deleted: . Without this type of data, satellite algorithms will continue to be biased towards the North Atlantic and mid-latitude regions…

Deleted: which, combined with the limited in-situ data, limits our understanding of the ecological and biogeochemical characteristics of the region.…

Deleted: ?

Deleted: Contrastingly

Deleted: concentration

Deleted: ?

combined with peak Chl *a* concentrations (Figure 2), reinforce the presence of a haptophyte bloom in this region. This represents a noteworthy deviation from community composition observations from the Western side of the Antarctic Peninsula where despite some exceptions (Trimborn et al., 2015), blooms are typically diatom- or cryptophyte-, not haptophyte-dominated (Brown et al., 2021).

Because the dominant haptophyte throughout the Southern Ocean is known to be *Phaeocystis antarctica* (*P. antarctica*; Smith and Trimborn, 2024), we presume that the enhanced proportional and discrete concentration of hex-fuco in this region corresponds to a high concentration of *P. antarctica*. Caution should be taken to assume all haptophytes represent *Phaeocystis antarctica*, but for the Larsen-C region, this assessment is supported by Flowcam data collected during the PICCOLO cruise sampling, which show the presence of *Phaeocystis* colonies (Fileman et al., 2026). Additionally, *P. antarctica* has been known to generate large blooms (both in spatial extent and biomass concentrations), leading to very high chlorophyll-*a* concentrations and rates of primary production (Smith et al., 2014; Meyer et al., 2025). The HPLC-derived concentrations of total chlorophyll *a* at Larsen C were the highest of any water column sample in this study, with a maximum concentration of 3.4 µg L^{-1} (Fig. 2A), representative of bloom concentrations. Total accessory pigment concentrations were similarly high (Figure S4). The Larsen C region also had the shallowest Secchi depth (6 m) and greenest water (Forel Ule colour of approximately 7) of any location during the campaign, consistent with a large *Phaeocystis* bloom.

The consistency in relative hex-fuco concentrations between samples that were collected at varying depths from 20-70 m is noteworthy (Figure 3). This result suggests that haptophytes (likely *P. antarctica*) dominated the community throughout the euphotic zone and supports previous findings, which describe *Phaeocystis* clades in general as cosmopolitan phytoplankton with a remarkable capacity to capitalize upon alleviation of resource limitation (Fussy et al., 2025). In the case of Larsen-C, alleviation of resource limitation likely corresponds to light and potential iron stress, as satellite imagery shows that the region had been sea-ice covered until a few days prior to sampling (Figure S1). Additionally, $\delta^{18}O$ analysis of seawater samples suggests the presence of ice shelf meltwater supplying dissolved iron to the region (Heywood and Bell, 2025). This region had previously been somewhat overlooked in importance due to a combination of lacking in situ data and ice-adjacency effects, which bias satellite-derived chlorophyll estimates (Oliver et al., 2025). However, the magnitude of the bloom (total chlorophyll-*a* concentrations > 3 µg L^{-1}) observed here, supports the conclusion of Oliver et al. (2025) that the Larsen-C Ice Shelf hosts one of the top 15 most productive polynyas in the Antarctic. Furthermore, our findings would suggest that a substantial amount of that primary production comes from haptophytes, like *P. antarctica*.

3.3 The Continental Shelf Community

Samples collected from the continental shelf (YD 34, 45, 47, 54-56, 61) had on average lower chlorophyll *a* (0.51 µg L^{-1}; Figure 2) and (0.41 µg L^{-1}; Figure S4) accessory pigment concentrations than those at Larsen-C but higher chlorophyll *a* and accessory pigment concentrations than the more offshore samples along the slope transect. Shelf samples had some of the highest percent contribution of fucoxanthin, particularly at 20 m and deeper where fucoxanthin dominated (32%), followed by chlorophyll c (22%; Figure 3G; 2I). This pigment composition resulted in diatom dominance in the *phytoclass* analysis from

Deleted:

Deleted: T

Formatted: Font: Italic

Deleted: ed

Deleted: S3

Deleted: ?

Deleted: .

Moved down [1]: The magnitude of the bloom (total chlorophyll-*a* concentrations > 3 µg L^{-1}) supports the conclusion of Oliver et al. (2025), derived from satellite imagery, that the Larsen-C Ice Shelf hosts one of the top 15 most productive polynyas in the Antarctic.

Deleted:

Deleted:

Deleted: n

Deleted:

Deleted: T

Deleted:), derived from satellite imagery,

Formatted: Font: Italic

Formatted: Font: Italic

Deleted: Samples collected from the continental shelf (YD 34, 45, 47, 54-56, 61) had on average lower (0.41 µg L^{-1}) accessory pigment concentrations than those at Larsen-C but higher accessory pigment concentrations than the more offshore samples along the slope transect (Figure ?).

Deleted: below

Deleted: 2

the deeper (50 – 100 m) shelf samples (Figure 3J-J). However, cryptophytes dominated (57%) at 20-49 m at one of the northernmost sampling locations (63.15 ºS, 52.74 ºW) on YD 54 and in the total size fraction surface sample on YD 61 (Figure 3). Interestingly, haptophytes dominated on YD 55 in both the 3 and 25 µm size fractions, but diatoms played a disproportionally larger role in the total sample (31% in the total vs. 8.1 and 9.4% in the 3 and 25 µm, respectively), suggesting that this station has a substantial population of large (>25 µm) diatoms (Figure 3C-D). The contrast between continental shelf and Larsen-C samples is noteworthy, with the shelf samples likely reflecting continental shelf community composition outside of bloom conditions. These "standard" conditions are more similar to that of the Ross Sea, another cold continental shelf sector, than to the West Antarctic Peninsula, a warm continental shelf sector (Thompson et al., 2018), which may suggest hydrography plays an important role in determining which species are most acclimated to dominate in the region. The rapid warming of the West Antarctic Peninsula is thought to contribute substantially to community composition changes in recent years (namely a shift from diatoms toward flagellates; Nardelli et al., 2023) whereas the colder temperatures and heavier ice concentrations common to the Weddell Sea likely enable the high concentrations of diatoms and haptophytes in the region.

3.4 The Slope Transect Community

The zonal transect spanned approximately 225 km across the continental slope from the shelf break to the open ocean environment of the Weddell Gyre (YD 39 – 45) . Despite this large longitudinal range, the pigment compositions from both the surface (<50 m; n = 6) and deeper water (>50 m; n = 5) were remarkably similar across the transect (Figure 3). Both depth ranges were dominated by fucoxanthin, hex-fuco, and chlorophyll c with percent concentrations ranging from 13-39%, 8-37%, and 5-23%, respectively (Figure 3). The homogeneity across samples suggests a consistent community composition in the slope region. This finding was further supported by *phytoclass* results, which showed the highest concentrations of diatoms (41%), followed by haptophytes (38%) and substantially smaller contributions from cryptophytes and *Synechococcus* (Figure 3). The consistency of the phytoplankton community is somewhat surprising given the changes in hydrography across the fronts in the slope region, suggesting that these hydrographic changes are not substantial controls on community composition within the region. Limited spatial variability appears to exist across the shelf to slope and continental shelf communities (Figure 3). This relative spatial homogeneity has also been hypothesized for the Ross Sea (Smith and Kaufman, 2018) but contrasts with what has been found along the West Antarctic Peninsula where changing water masses heavily influence temperature and nutrient concentrations and create substantial shifts in community composition latitudinally and from the near coast to shelf-slope regions (Moreno et al., 2024).

The contrast between community composition at Larsen-C and the slope transect is noteworthy when considering the foodweb dynamics of the region. Typically, diatoms are thought to support shorter, more efficient foodwebs (Michaels and Silver, 1988) while smaller cells such as cryptophytes and *Synechococcus* are thought to contribute to longer foodwebs with higher rates of recycling and more energy loss (Schmidt et al., 2020). Additionally, *P. antarctica* colonies are thought to be unpalatable for many krill and zooplankton species (Caron et al., 2000; Smith et al., 2014), leading to disruptions in the Antarctic food chain. The relative dominance of *P. antarctica* in our Larsen-C samples suggests that there are likely substantial,

Deleted: 2

Deleted: ?

Deleted: ?

Deleted: .

Deleted: s

Deleted: 2

Deleted: shelf-

Deleted: 2

Deleted: The relative homogeneity

Deleted: is

Deleted: consistent with homogeneity of the phytoplankton community across the continental shelf, as has been

Deleted: the influence of spatial gradients for differing community composition appear large

Deleted: shelf-

spatiotemporal differences between the Larsen-C region and the rest of the Weddell Sea in terms of zooplankton grazing, nutrient cycling, and carbon export. Further research should investigate whether *P. antarctica* blooms commonly occur across the Weddell Sea as sea ice retreats and additional polynyas form. Understanding how frequently these blooms occur and quantifying the associated increases in *P. antarctica*, particularly relative to diatom concentrations, would help better quantify regional primary production and carbon export rates.

3.5 The Sea Ice Community

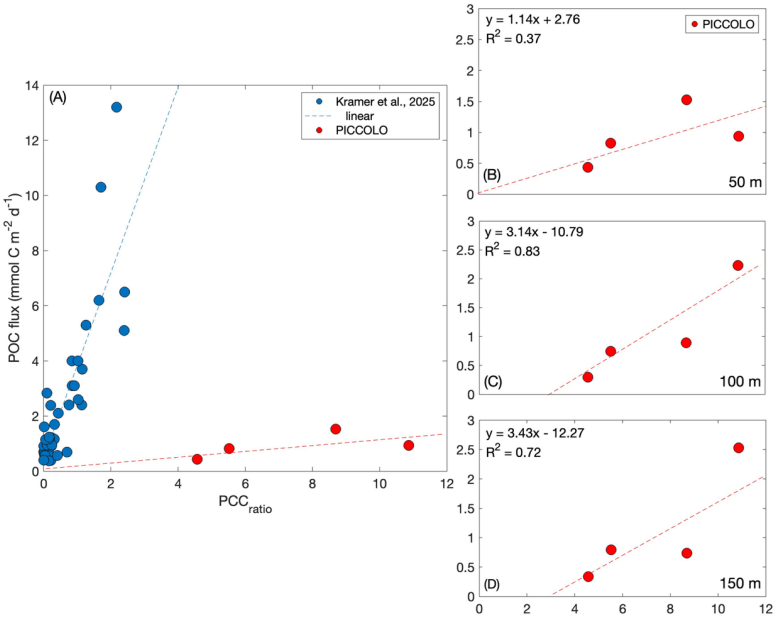
The six samples collected from sea-ice cores (n = 2; YD 57-58), the ice-ocean interface (n = 2; YD 57-58), and brown ice (n = 2; YD 56) had extremely high concentrations of chlorophyll *a* (29 – 42 µg L^{-1}; Figure 2F) and total accessory pigments (Figure S4), which was predominantly fucoxanthin (ranging from 11 - 66%), particularly in the brown ice samples (Figure 3K). Alloxanthin and chlorophyll c also contributed substantially, ranging from 0 - 42% and 16 – 23%, respectively. This pigment composition led to a clear prevalence of diatoms in the *phytoclass* results (Figure 3L). Cryptophytes were also an important proportion of the community, particularly in the ice-ocean interface samples. These findings show a noteworthy difference in community composition between sample types despite the fact that the two communities coexist in the same geographic space, i.e., near complete dominance of diatoms in core samples whereas ice-ocean samples have a more mixed composition (Figure 3K-L). As has been previously shown, sea-ice dwelling diatoms, and to some degree cryptophytes, must have unique physiological or adaptive traits to enable them to survive in colder, less saline, and less viscous environments (Ligowski et al., 2012). The difference we found in community composition between the sea-ice community and all other samples (Figure 3) suggests that ice or ice-adjacent communities should be considered independently from open water communities in models and climatologies.

3.6 POC Flux vs. Community Composition

POC flux at 50, 100, and 150 m shows positive but non-significant linear relationships with surface (<10 m) community composition PCC_{ratio} (Figure 4). Interestingly, the relationship was weakest (R^2 = 0.37) at 50 m, the shallowest depth, but strongest (even stronger than the relationship observed by Kramer et al. (2025)), at 100 m (R^2 = 0.83; Figure 4C) which is a depth of enhanced krill grazing and faecal pellet production (Atherden et al., 2026), leading to enhanced POC flux. Regardless of the depth of POC flux evaluated in this study, the observed relationship is substantially different from that reported by Kramer et al. (2025), where PCC_{ratio} values were much lower but rates of POC flux were much higher. This deviation is likely due to substantial ecological and biogeochemical differences between the Southern Ocean relative to the North Pacific and the North Atlantic. Specifically, the Antarctic continental shelf is known to be dominated by a mixed assemblage of diatoms, *P. antarctica*, and cryptophytes (Wright et al., 2010; Hayward et al., 2025) while the North Pacific and the North Atlantic are dominated by much more mixed assemblages of dinoflagellates, diatoms, haptophytes, chlorophytes, and *Synechococcus* (Sharpe et al., 2023; Meyer et al., 2024; Kramer et al., 2025). Therefore, it is unsurprising that our PCC_{ratio} values were all >1 and much larger (4.6 – 11) than those of Kramer et al. (2025). Contrastingly, the rates we determined for

Deleted: 3
Deleted: 2
Deleted: 2
Deleted: live
Deleted: 2
Deleted: 2
Deleted: The
Deleted: vs. PCC_{ratio}
Deleted: between
Deleted: and carbon export at 50, 100, and 150 m
Deleted: 3
Formatted: Subscript
Deleted: 3
Deleted: No matter
Deleted: export
Deleted: Southern Ocean
Deleted: of

POC flux were lower than those found by Kramer et al. (2025). The dominance of diatoms, haptophytes, and cryptophytes lead to high PCC_{ratio}, but some studies suggest that a substantial proportion of *Phaeocystis* is remineralized in the surface, reducing the rates of POC flux to depth (Meyer et al., 2022). These differences in ecosystem characteristics between Kramer et al. (2025) and our study, along with the limited number of northwest Weddell Sea samples, necessitate different linear equations to describe the relationship between community composition and carbon export. The substantial ecological differences between the Kramer et al. (2025) dataset and this study highlight the potential utility of this relationship to predict the magnitude of POC flux across diverse ecosystems. While further in situ Antarctic sampling and analysis is clearly required, even the limited number of samples shown here suggest that a strong relationship exists. Critically, unique linear regression coefficients should be derived to calculate export in highly different ecological regions, or at least polar versus non-polar regions.



Deleted: carbon export

Deleted:

Deleted: this

Deleted:

Deleted: ,

Deleted:

Figure 4. POC flux (mmol C m^{-2} d^{-1}) versus the contribution of diatoms and hacrobia to phytoplankton community composition (PCC_{ratio}) in the surface (>20 m). (A) includes HPLC and 50 m sediment trap data from the PICCOLO campaign compared to data from Kramer et al. (2025). (B-D) present PICCOLO HPLC and sediment trap data from 50, 100, and 150 m, respectively. The R^2 values for (B-D) are 0.37, 0.83, and 0.72, respectively, and p-values were > 0.05 for all relationships.

The water overlying the four floating trap stations presented here was dominated by diatoms with percent contributions of 84, 61, 72, and 60% compared with the haptophyte percent contributions of 13, 20, 12, and 2% for YD 35 (shelf sample), YD 39 (transect), YD 47 (shelf sample), and YD 57 (ice sample), respectively. To test whether diatom abundance alone could be used as a indicator of POC flux (i.e., carbon export) in the euphotic zone, the percent contribution of just diatoms was regressed against POC flux (Figure S5). At 50, 100, and 150 m, the R^2 values decreased substantially from those of PCC_{ratio} to 0.01, 0.06, and 0.08, respectively. R^2 values were similarly weak if just haptophytes or just cryptophytes were regressed versus carbon export (0.10, 0.01, and 0.01 for haptophytes at 50, 100, and 150 m and 0.03 and 0 for cryptophytes at 100 and 150 m; Figure S5). The one exception to this finding was the relationship between percent contribution of cryptophytes to carbon export at 50 m, which had an exceptionally high R^2 value of 0.93 (*P*-value < 0.05; Figure S5). With this relationship, and all the presented relationships, caution should be taken given the small sample size (n = 4). However, this result suggests that it is not solely the relative diatom, haptophyte, or cryptophyte abundances that are a good predictor of carbon export, but that diatoms + hacrobia together are the most robust metric at multiple depths and should be evaluated together against POC flux in remote sensing products and global models.

While some previous studies have shown that diatoms are highly correlated with carbon export due to their fast sinking rates and potential to be readily grazed (Michaels and Silver 1988; Zuniga et al., 2021; Siegel et al., 2025), other studies (Cassar et al., 2015; Williams et al., 2024) have found that diatoms are not always a good indicator of export efficiency (i.e., the proportion of POC that gets exported to depth) in the Southern Ocean. Our results support a growing body of evidence which suggests that the balance between diatoms and *Phaeocystis* is critical for determining the magnitude of both primary production and carbon export rates globally. Numerous studies (Smith et al., 1991; Meyer et al., 2022; Smith and Trimborn, 2024; Meyer et al., 2025; Roca-Marti et al., 2025) have found that *Phaeocystis sp.* contributes to high rates of primary production, but the high remineralization rate of *Phaeocystis* in the surface ocean means that rates of production become uncoupled from export rates, keeping export rates low or consistent with non-bloom conditions. Unfortunately, due to limited trap deployments, we could not directly assess the relationship between phytoplankton community composition and POC flux during the *Phaeocystis* bloom but suggest that this should be investigated in future Antarctic field campaigns. Furthermore, cryptophytes have not been as large a focus as diatoms or *Phaeocystis* in Southern Ocean carbon export analyses, but our results suggest that they too play a large, perhaps overlooked, role in carbon flux. Typically, cryptophytes have been believed to shorten food webs and decrease carbon flux and are frequently mixotrophic (Brown et al., 2021), so overlooking these organisms in models could potentially lead to overestimates of flux.

Deleted: 3
Deleted: s
Deleted: plots
Deleted: predictor
Deleted: carbon export
Deleted: 4
Deleted: 4
Deleted: 4
Deleted:
Formatted: Font: Italic

More concurrent in situ community composition and carbon export observations are needed to better test the relationships found here within the Weddell Sea continental shelf and the wider Southern Ocean. The robustness of the relationships shown here and by Kramer et al. (2025) should be further tested in space and time in order to evaluate this potentially predictive relationship between PCC_{ratio} measured from next generation ocean colour satellite products and POC flux (Kramer et al., 2022).

4 Conclusions

As one of the only HPLC datasets from the Weddell Sea continental shelf, this study presents valuable observations to characterise the phytoplankton community and how it relates to the magnitude of POC flux in this region. We confirmed an expected dominance of diatoms and haptophytes throughout the region. We presented new geographic and depth patterns that highlight understudied phytoplankton community dynamics such as the stable contribution of haptophytes (presumably *P. antarctica*) in the surface and at depth during a bloom, the higher contribution of cryptophytes in surface waters relative to depth, the low cryptophyte abundance in haptophyte dominated waters, and the overwhelming dominance of diatoms in sea-ice samples. The results presented here showcase the importance of understanding variable phytoplankton community composition and show a strong positive relationship between POC flux and high proportions of diatoms, typically thought to enhance flux, and hacrobia, typically thought to reduce flux. The contrast of the expected impacts diatoms and haptophytes have on flux, as well as the importance of cryptophytes, highlights the complexity of the relationship between phytoplankton community composition and carbon cycle processes.

While more research is needed to robustly test this relationship through space and time, particularly in multiple bloom stages and during a *Phaeocystis* bloom, the potential predictive capacity of diatom + photosynthetic hacrobia community composition to estimate the magnitude of POC flux appears strong and holds across oceanic systems. Currently, some Earth Systems models have begun to differentiate between key phytoplankton groups like diatoms and *Phaeocystis* (Enright et al., 2009), but not all. Our findings suggest that including key hacrobia, such as *Phaeocystis* and cryptophytes, as independent groups in Earth System models is a key step in developing a more comprehensive, mechanistic understanding of the relationship between changing phytoplankton community composition and key ecosystem and biogeochemical processes, particularly in critical areas such as the Weddell Sea and Southern Ocean.

Code and data availability

Deleted: s

Deleted: This study presents

Deleted:

Deleted: (to our knowledge)

Deleted: decrease of

Deleted:

Deleted: ,

Deleted: strong

Deleted: predictive

Formatted: Font: Italic

Deleted: e

Deleted: s

Deleted: m

HPLC data are available at the British Oceanographic Data Centre (https://doi.org/10.5285/4D5D158B-3CF9-AD21-E063-7086ABC01540), and POC flux data are at the British Oceanographic Data Centre (https://doi.org/10.5285/47f15a7a-de57-dc68-e063-7086abc0ccb7).

Deleted: All data

Deleted: .

Author contributions

MGM is responsible for conceptualisation, data curation, formal analysis, investigation, validation, visualisation, writing (original draft preparation), and writing (review and editing). RJWB, XS, CM, FA, and GD are responsible for data curation, methodology, validation, visualisation, writing (original draft preparation), and writing (review and editing). SJK is responsible for conceptualisation, methodology, validation, writing (original draft preparation), and writing (review and editing). KJH is responsible for validation, visualisation, resources, project administration, writing (original draft preparation), and writing (review and editing).

Competing interests

K. Heywood is an editor of Ocean Science.

Disclaimer

Copernicus Publications remains neutral with regard to jurisdictional claims made in the text, published maps, institutional affiliations, or any other geographical representation in this paper. While Copernicus Publications makes every effort to include appropriate place names, the final responsibility lies with the authors. Views expressed in the text are those of the authors and do not necessarily reflect the views of the publisher.

Acknowledgements

We thank everyone associated with cruise SD035 on the RRS Sir David Attenborough. This work is part of the PICCOLO (Processes Influencing Carbon Cycling: Observations of the Lower limb of the Antarctic Overturning) project. Additionally, we thank Rob Utting and Elise Brabben for their help in facilitating shipping and analysis of the HPLC samples.

Financial support

The PICCOLO project was supported by Natural Environment Research Council Grants NE/P021395/1 (MGM and KJH) and NE/P021352/1 (CM and FA)). CM was supported by UKRI FLF CUPIDO (MR/T020962). RB and XS were supported by a

Deleted: (

Deleted: .

UKRI FLF grant (MR/V022792/1). XS was supported by the Collaborative Antarctic Science Scheme (CASS, British Antarctic Survey, 2023/24 season). SJK was supported by NASA Ocean Biology and Biogeochemistry grant 80NSSC25K7428. GD was funded by the European Union (101083922) and UKRI under the UK government's Horizon Europe funding guarantee (10054454, 10063673, 10064020, 10059241, 10079684, 10059012, 10048179).

Deleted:

Deleted: (

Deleted:)

Deleted:)

References

Anderson, S.I., Barton, A.D., Clayton, S., Dutkiewicz, S., and Rynearson, T.A.: Marine phytoplankton functional types exhibit diverse responses to thermal change. Nature 12, 6413. doi.org/10.1038/s41467-021-26651-8. 2021.

Atherden, F.S., Rowlands, E., Flint, G., Fielding, S., Schmidt, K., Fileman, E., Atkinson, A., and Manno, C. Krill defecation at depth reduced carbon flux attenuation in the Weddell Sea euphotic zone. Ocean Science. doi.org/10.5194/egusphere-2026-988. 2026.

Bracher, A., Bouman, H.A., Brewin, R.J.W., Bricaud, A., et al. Obtaining phytoplankton diversity from ocean color: A scientific roadmap for future development. Frontiers in Marine Science 4. doi.org/10.3389/fmar.2017.00055. 2017.

Brown, M.S., Bowman, J.S., Lin, Y., Feehan, C.J., Moreno, C.M., Cassar, N., Marchetti, A., and Schofield, O.M. Low diversity of a key phytoplankton group along the West Antarctic Peninsula. Limnology and Oceanography 66, 2470-2480. doi.org/10.1002/lno.11765. 2021.

Brown, M.S., Munro, D.R., Feehan, C.J., Sweeney, C., Ducklow, H.W., and Schofield, O.M. Enhanced oceanic CO_2 uptake along the rapidly changing West Antarctic Peninsula. Nature Climate Change 9, 678-683. doi.org/10.1038/s41558-019-0552-3. 2019.

Cael, B.B., Dutkiewicz, S., and Henson, S. Abrupt shifts in 21st-century plankton communities. Science Advances 7(44). doi.org/10.1126/sciadv.abf8593. 2021.

Caron, D.A., Dennett, M.R., Lonsdale, D.J., Moran, D.M., and Shalapyonok, L. Microzooplankton herbivory in the Ross Sea, Antarctica. Deep-Sea Research II, 47(15-16), 3249-3272. doi.org/10.1016/S0967-0645(00)00067-9. 2000.

Cassar, N., Wright, S.W., Thomson, P.G., Trull, T.W., Westwood, K.J., de Salas, M., Davidson, A., Pearce, I., Davies, D.M., & Matear, R.J. The relation of mixed-layer net community production to phytoplankton community composition in the Southern Ocean. Global Biogeochemical Cycles 29(4), 446-462. doi.org/10.1002/2014GB004936. 2015.

Cetinic, I., Rousseaux, C.S., Carroll, I.T., Chase, A.P., et al. Phytoplankton composition from sPACE: Requirements, opportunities, and challenges. Remote Sensing of Environment 302, 113964. doi.org/10.1016/j.rse.2023.113964. 2024.

Chase, A.P., Boss, E., Cetinic, I., and Slade, W. Estimation of phytoplankton accessory pigments from hyperspectral reflectance spectra: Towards a global algorithm. Journal of Geophysical Research 122(12), 9725-9743. doi.org/10.1002/2017JC012859. 2017.

Chen, S., Smith, W.O., Jr., and Yu, X. Revisiting the ocean color algorithms for particulate organic carbon and chlorophyll-a concentrations in the Ross Sea. Journal of Geophysical Research Oceans 126(8). doi.org/10.1029/2021JC017749.

Deppeler, SL, & Davidson, AT. 2017. Southern Ocean phytoplankton in a changing climate. Frontiers in Marine Science 4. doi.org/10.3389/fmars.2017.00040. 2021.

Enright, C., Buitenhuis, E., Vogt, M., and Le Quere, C. PlankTOM10 User Manual Version 1.02. 2009.

Fileman, E., Mohideen, K, & Tarran, GA. 2026. Abundance of Protists measured from the water column beneath two sea-ice floes in the Weddell Sea during the PICCOLO research cruise SD035 in January-March 2024. NERC EDS British Oceanographic Data Centre NOC. doi:10.5285/47b5aaed-7bda-4f73-e063-7086abc0e5a0.

Flynn, RF, Haraguchi, L., McQuaid, J., Burger, J.M., Lunga, P.M., Stirnimann, L., Samanta, S., Roychoudhury, A.N., and Fawcett, S.E. Nanoplankton: The dominant vector for carbon export across the Atlantic Southern Ocean in spring. Science Advances 9(48). doi.org/10.1126/sciadv.adi3059. 2023.

Fussy, Z., Lampe, R.H., Arrigo, K.R., Barry, K., et al. Genome-resolved biogeography of Phaeocystales, cosmopolitan bloom-forming algae. Nature communications 16:8559. doi.org/10.1038/s41467-025-63565-1. 2025.

Gorman, E.T., Kubalak, D.A., Patel, D., Dress, A., Mott, D.B., Meister, G., and Werdell, P.J. The NASA Plankton, Aerosol, Cloud, ocean Ecosystem (PACE) mission: an emerging era of global, hyperspectral Earth system remote sensing. Sensors, Systems, and Next-Generation Satellites XXIII. doi.org/10.1117/12.2537146. 2019.

Hayward, A., Pinkerton, M.H., and Gutierrez-Rodriguez, A. Phytoclass: A pigment-based chemotaxonomic method to determine the biomass of phytoplankton classes. Limnology and Oceanography: Methods 21, 220-241. doi.org/10.1002/lom3.10541. 2023.

Hayward, A., Pinkerton, M.H., Wright, S.W., Gutierrez-Rodrigues, A., and Law, C.S. Twenty-size years of phytoplankton pigments reveal a circumpolar class divide around the Southern Ocean. Communications Earth and Environment 5(92). doi.org/10.1038/s43247-024-01261-6. 2024.

Hayward, A., Wright, S.W., Carroll, D., Law, C.S., Wongpan, P., Gutierrez-Rodriguez, A., and Pinkerton, M.H. Antarctic phytoplankton communities restructure under shifting sea-ice regimes. Nature Climate Change. doi.org/10.1038/s41558-025-02379-x. 2025.

Henson, S.A., Cael, B.B., Allen, S.R., and Dutkiewicz, S. Future phytoplankton diversity in a changing climate. Nature Communications 12(5372). doi.org/10.1038/s41467-021-25699-w. 2021.

Heywood, K.., Bell, T. et al. RRS *Sir David Attenborough* cruise SD035, 17 January – 08 March 2024. PICCOLO cruise report 347pp. 2024.

Hong, Z., Long, D., Shan, K., Zhang, J., Woolway, R.I., Liu, M., Mann, M.E. and Fang, H. Declining ocean greenness and phytoplankton blooms in low to mid-latitudes under a warming climate. Science Advances 11(42). doi.org/10.1126/sciadv.adx4857. 2025.

Kang, S-.H., and Fryxell, G.A. Phytoplankton in the Weddell Sea, Antarctica: composition, abundance and distribution in water-column assemblages of the marginal ice-edge zone during austral autumn. Marine Biology 116, 335-348. doi.org/10.1007/BF00350024. 1993.

Kramer, S.J., Bolanos, L.M., Catlett, D., Chase, A.P., et al. Towards a synthesis of phytoplankton community composition methods for global-scale application. Limnology and Oceanography 22(4), 217-240. doi.org/10.1002/lom3.10602. 2024.

Kramer, S. J., E. L. Jones, M. L. Estapa, N. L. Paul, T. A. Rynearson, A. E. Santoro, S. Sudek, and C. A. Durkin. Sinking particles exporting diatoms and hacrobia predict the magnitude of oceanic POC flux. The ISME Journal wraf105. doi:10.1093/ismejo/wraf105. 2025.

Kramer, S.J., and Siegel, D.A. How can phytoplankton pigments be best used to characterize surface ocean phytoplankton groups for ocean color remote sensing algorithms. Journal of Geophysical Research 124(11), 7557-7574. doi.org/10.1029/2019JC015604. 2019.

Kramer, S.J., Siegel, D.A., Maritorena, S., and Catlett, D. Modeling surface ocean phytoplankton pigments from hyperspectral remote sensing reflectance on global scales. Remote Sensing of Environment 270, 112879. doi.org/10.1016/j.rse.2021.112879. 2022.

Le Quere, C., Harrison, S.P., Prentice, I.C., Buitenhuis, Aumont, O., et al. Ecosystem dynamics based on plankton functional types for global ocean biogeochemistry models. Global Change Biology 11, 2016-2040. 2005.

Ligowski, R., Jordan, R.W., and Assmy, P. Morphological adaptation of a planktonic diatom to growth in Antarctic sea ice. Marine Biology 159, 817-827. doi.org/10.1007/s00227-011-1857-6. 2012.

Lin, Y., Gifford, S., Ducklow, H., Schofield, O., and Cassar, N. Towards quantitative microbiome community profiling using internal standards. Applied and Environmental Microbiology 85(5). doi.org/10.1128/AEM.02634-18. 2019.

Lin, Y., Moreno, C., Marchetti, A., Ducklow, H., Schofield, O., Delage, E., Meredith, M., Li, Z., Eveillard, D., Chaffron, S., and Cassar, N. Decline in plankton diversity and carbon flux with reduced sea ice extent along the Western Antarctic Peninsula. Nature Communications 12, 4948. doi.org/10.1038/s41467-021-25235-w. 2021.

Mackey, M.D., Mackey, D.J., Higgins, H.W., and Wright, S.W. CHEMTAX- a program for estimating class abundances from chemical markers: application to HPLC measurements of phytoplankton. Marine Ecology Progress Series 144, 265-283. doi.org/10.3354/meps144265. 1996.

Mendes, C.R.B., Tavano, V.M., Kerr, R., Dotto, T.S., Maximiano, T., and Secchi, E.R. Impact of sea ice on the structure of phytoplankton communities in the northern Antarctic Peninsula. Deep Sea Research 149, 111-123. doi.org/10.1016/j.dsr2.2017.12.003. 2018.

Meyer, M.G., Jones, R.M., and Smith, W.O., Jr. Quantifying seasonal particulate organic carbon concentrations and export potential in the southwestern Ross Sea using autonomous gliders. Journal of Geophysical Research Oceans 127. doi.org/10.1029/2022JC018798. 2022.

Meyer, M.G., Brzezinski, M.A., Cohn, M.R., Kramer, S.J., Paul, N., Sharpe, G., Niebergall, A.K., Gifford, S., Cassar, N., and Marchetti, A. Size-fractionated primary production dynamics during the decline phase of the North Atlantic spring bloom. Global Biogeochemical Cycles 38. doi.org/10.1029/2023GB008019. 2024.

731 Meyer, M.G., Portela, E., Smith, W.O. Jr, and Heywood, K.J. Critical uncoupling between biogeochemical stocks and rates in
732 Ross Sea springtime production-export dynamics. Ocean Science 21, 1223-1236. doi.org/10.5194/os-21-1223-
733 2025. 2025.
734 Michaels, A.F., and Silver, M.W. Primary production, sinking fluxes, and the microbial food web. Deep-Sea Research 35(4),
735 473-490. doi.org/10.1016/0198-0149(88)90126-4. 1988.
736 Moreno, C.M., Bernish, M., Meyer, M.G., Li, Z., Waite, N., Cohen, N.R., Schofield, O., and Marchetti, A. Molecular
737 physiology of Antarctic diatom natural assemblages and bloom event reveal insights into strategies contributing to
738 their ecological success. mSystems 9(3). doi.org/10.1128/msystems.01306-23. 2024.
739 Nardelli, S.C., Gray, P.C., Stammerjohn, S.E., and Schofield, O. Characterizing coastal phytoplankton seasonal succession
740 patterns on the West Antarctic Peninsula. Limnology and Oceanography 68(4), 845-861.
741 doi.org/10.1002/lno.12314. 2023.
742 Oliver, H., Turner, J.S., Castagna, A., Houskeeper, H., and Dierssen, H. High Antarctic coastal productivity in polynyas
743 revealed by considering remote sensing ice-adjacency effects. Limnology and Oceanography Letters,
744 doi.org/10.1002/lol2.70043. 2025.
745 Roca-Marti, M., Healey, M., McBride, C.E., Sipler, R., Devred, E., Cisternas-Novoa, C., Romanelli, E., Ohashi, K., and
746 Kienast, S.S. Sinking particle fluxes and biological carbon pump efficiency in the Labrador Sea during a Phaeocystis
747 bloom decline. EGUsphere, preprint. doi.org/10.5194/egusphere-2025-3671. 2025.
748 Sathyendranath, S. Reports and monographs of the international ocean-colour coordinating group. IOCCG Report Number 15.
749 2014.
750 Schloss, I., and Estrada, M. Phytoplankton composition in the Weddell-Scotia Confluence area during austral spring in relation
751 to hydrography. Polar Biology 14, 77-90. doi.org/10.1007/BF00234969. 1994.
752 Sharpe, G., Zhao, L., Meyer, M.G., Gong, W., Burns, S.M., Tagliabue, A., Buck, K.N., Santoro, A.E., Graff, J.R., Marchetti,
753 A., and Gifford, S. Synechococcus nitrogen gene loss in iron-limited ocean regions. ISME Communications 3(1).
754 doi.org/10.1038/s43705-023-00314-9. 2023.

Smith, R.C., Baker, K.S., Fraser, W.R., Hofmann, E.E., Karl, D.M., Klinck, J.M., Quentin, L.B., Prezelin, B.B., Ross, R.M., Trivelpiece, W.Z., and Vernet, M. The Palmer LTER: A Long-Term Ecological Research Program at Palmer Station, Antarctica. Oceanography 8(3), 77-86. 1995.

Smith, W.O., Jr., Ainley, D.G., Arrigo, K.R., and Dinniman, M.S. The oceanography and ecology of the Ross Sea. Annual Review of Marine Science 6(1), 469-487. doi.org/10.1146/annurev-marine-010213-135114. 2014.

Smith, W.O., Jr., Codispoti, L.A., Nelson, D.M., Manley, T., Buskey, E.J., Niebauer, H.J., and Cota, G.F. Importance of Phaeocystis blooms in the high-latitude ocean carbon cycle. Nature 352, 514-516. doi.org/10.1038/352514a0. 1991.

Smith, W.O., Jr., and Kaufman, D.E. Climatological temporal and spatial distributions of nutrients and particulate matter in the Ross Sea. Progress in Oceanography 168, 182-195. doi.org/10.1016/j.pocean.2018.10.003. 2018.

Smith, WO., Jr., and Trimborn, S. Phaeocystis: A global enigma. Annual Review of Marine Science 16, 417-441. doi.org/10.1146/annurev-marine-022223-025031. 2024.

Suomalainen, J., Oliviera, R.A., Hakala, T., Koivumaki, N., Markelin, L., Nasi, R., and Honkavaara, E. Direct reflectance transformation methodology for drone-based hyperspectral imaging. Remote Sensing of Environment 266. Doi.org/10.1016/j.rse.2021.112691. 2021.

Thomalla, S.J., Nicholson, S.-A., Ryan-Keogh, T.J., and Smith, M.E. Widespread changes in Southern Ocean phytoplankton blooms linked to climate drivers. Nature Climate Change 13, 975-984. doi.org/10.1038/s41558-023-01768-4. 2023.

Thompson, A.F., Stewart, A.L., Spence, P., and Heywood, K.J. The Antarctic slope current in a changing climate. Reviews of Geophysics 56, 741-770. doi.org/10.1029/2018RG000624. 2018.

Trimborn, S., Hoppe, C.J.M., Taylor, B.B., Bracher, A., and Hassler, C. Physiological characteristics of open ocean and coastal phytoplankton communities of Western Antarctic Peninsula and Drake Passage waters. Deep Sea Research 98, 115-124. doi.org/10.1016/j.dsr.2014.12.010. 2015.

Van Heukelem, L. and Thomas, C. Computer assisted high-performance liquid chromatography method development with applications to the isolation and analysis of phytoplankton pigments. J. Chromatogr. A. 910: 31-49. 2001.

Venables, H., Meredith, M.P., Hendry, K.R., ten Hoopen, P., Peat, H., et al. Sustained year-round oceanographic measurements from Rothera Research Station, Antarctica, 1997-2017. Scientific Data 10(265). doi.org/10.1038/s41597-023-02172-5. 2023.

von Berg, L., Prend, C.J., Campbell, E.C., Mazloff, M.R., Talley, L.D., & Gille, S.T. Weddell Sea phytoplankton blooms modulated by sea ice variability and polynya formation. Geophysical Research Letters 47. doi.org/10.1029/2020GL087954. 2020.

Williams, J.R., Giering, S.L.C., Baker, C.A., Pabortsava, K., Briggs, N., East, H., Espinola, B., Blackbird, S., Le Moigne, F.A.C., Villa-Alfageme, M., Poulton, A.J., Carvalho, F., Pebody, C., Saw, K., Moore, C.M., Henson, S.A., Sanders, R., and Martin, A.P. Inefficient transfer of diatoms through the subpolar Southern Ocean twilight zone. Nature Geoscience 18, 72-77. doi.org/10.1038/s41561-024-01602-2. 2024.

Wright, S.W., van den Enden, R.L., Pearce, I., Davidson, A.T., Scott, F.J., and Westwood, K.J. Phytoplankton community structure and stocks in the Southern Ocean (30-80ºE) determined by CHEMTAX analysis of HPLC pigment signatures. Deep-Sea Research II 57, 758-788. doi.org/10.1016/j.dsr2.2009.06.015. 2009.

Xi, H., Bretagnon, M., Mehdipour, E., Demaria, J., Mangin, A., and Bracher, A. Consistent long-term observations of surface phytoplankton functional types from space. Scientific Synthesis Reports and Assessments 7, doi.org/10.5194/sp-6-osr9-7-2025. 2025.

Xi, H., Losa, S.N., Mangin, A., Soppa, M., Garnesson, P., Demaria, J., Liu, Y., d'Andon, O.H.F., and Bracher, A. Global retrieval of phytoplankton functional types based on empirical orthogonal functions using CMEMS GlobColour merged products and further extension to OLCI data. Remote Sensing of Environment 240. doi.org/10.1016/j.rse.2020.111704. 2020.

Zuniga, D., Sanchez-Vidal, A., Flexas, M.M., Carroll, D., Rufino, M.M., Spreen, G., Calafat, A., and Abrantes, F. Sinking diatom assemblages as a key driver for deep carbon and silicon export in the Scotia Sea (Southern Ocean). Frontiers in Earth Science 9. doi.org/10.3389/feart.2021.579198. 2021.